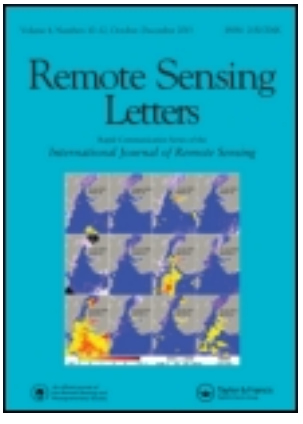

Remote Sensing Letters
Publication details, including instructions for authors and subscription information:
http://www.tandfonline.com/loi/trsl20

Derivation of a tasselled cap transformation based on Landsat 8 at-satellite reflectance

Muhammad Hasan Ali Baig[ab], Lifu Zhang[a], Tong Shuai[ab] & Qingxi Tong[a]

[a] State Key Laboratory of Remote Sensing Sciences, Institute of Remote Sensing and Digital Earth (RADI), Chinese Academy of Sciences, Beijing, China

[b] University of Chinese Academy of Sciences, Beijing, China

Published online: 06 Jun 2014.

To cite this article: Muhammad Hasan Ali Baig, Lifu Zhang, Tong Shuai & Qingxi Tong (2014) Derivation of a tasselled cap transformation based on Landsat 8 at-satellite reflectance, Remote Sensing Letters, 5:5, 423-431, DOI: 10.1080/2150704X.2014.915434

To link to this article: http://dx.doi.org/10.1080/2150704X.2014.915434

Remote Sensing Letters, 2014
Vol. 5, No. 5, 423–431, http://dx.doi.org/10.1080/2150704X.2014.915434

Taylor & Francis
Taylor & Francis Group

Derivation of a tasselled cap transformation based on Landsat 8 at-satellite reflectance

Muhammad Hasan Ali Baig[a,b], Lifu Zhang[a]*, Tong Shuai[a,b], and Qingxi Tong[a]

[a]*State Key Laboratory of Remote Sensing Sciences, Institute of Remote Sensing and Digital Earth (RADI), Chinese Academy of Sciences, Beijing, China;* [b]*University of Chinese Academy of Sciences, Beijing, China*

(*Received 6 February 2014; accepted 12 April 2014*)

The tasselled cap transformation (TCT) is a useful tool for compressing spectral data into a few bands associated with physical scene characteristics with minimal information loss. TCT was originally evolved from the Landsat multi-spectral scanner (MSS) launched in 1972 and is widely adapted to modern sensors. In this study, we derived the TCT coefficients for the newly launched (2013) operational land imager (OLI) sensor on-board Landsat 8 for at-satellite reflectance. A newly developed standardized mechanism was used to transform the principal component analysis (PCA)-based rotated axes through Procrustes rotation (PR) conformation according to the Landsat thematic mapper (TM)-based tasselled cap space. Firstly, OLI data were transformed into TM TCT space directly and considered as a dummy target. Then, PCA was applied on the original scene. Finally, PR was applied to get the transformation results in the best conformation to the target image. New coefficients were analysed in detail to confirm Landsat 8-based TCT as a continuity of the original tasselled cap idea. Results show that newly derived set of coefficients for Landsat OLI is in continuation of its predecessors and hence provide data continuity through TCT since 1972 for remote sensing of surface features such as vegetation, albedo and water. The newly derived TCT for OLI will also be very useful for studying biomass estimation and primary production for future studies.

1. Introduction

Vegetation and water indices derived from satellite reflectance data are two of the primary sources of information for operational monitoring of the Earth's land cover. Almost all the present vegetation indices (VIs) in remote sensing combine reflectance measurements from different portions of the electromagnetic spectrum to provide information about vegetation coverage on the ground. One of the primary applications of remote sensing is to identify patterns of vegetation distribution on the ground followed by assessing temporal changes in vegetation. Higher reflectance of vegetation and lower reflectance of water in near infrared (NIR) band along with different spectral responses of various vegetation types from visible to shortwave infrared (SWIR) led researchers to develop numerous indices (Jackson and Huete 1991; Richardson and Everitt 1992; Richardson and Wiegand 1977). Such indices are based on different algebraic combinations of these bands for proper analysis of land features. In contrast to its higher reflectance in NIR, vegetation has low reflectance in both the blue and the red regions of the spectrum due to absorption by chlorophyll for photosynthesis. These are the reasons why most of the traditional

*Corresponding author. Email: zhanglf@radi.ac.cn

vegetation indices are based on red–NIR space while using an inclined red–NIR line in red–NIR space as the line of zero vegetation for bare soil (Ray 1994; Viña et al. 2011; Payero, Neale, and Wright 2004; Bannari et al. 1995; Gitelson et al. 2002). Based on this soil line, vegetation indices can be divided into three categories: the slope-based VIs (e.g. Normalized Difference Vegetation Index – NDVI, Soil Adjusted Vegetation Index – SAVI and Ratio Vegetation Index – RVI, etc.), the distance-based (or perpendicular line) VIs (e.g. Perpendicular Vegetation Index-PVI, Difference Vegetation Index-DVI and Weighted Difference Vegetation Index-WDVI, etc.) and the orthogonal transformation VIs (such as Vegetation Index based on Universal Pattern Decomposition Index – VIUPD, etc.) (Richardson and Everitt 1992; Huete 1988; Clevers 1988; Huete, Jackson, and Post 1985; Richardson and Wiegand 1977; Rouse et al. 1973; Jordan 1969; Zhang et al. 2007). The tasselled cap transformation (TCT) belongs to the category of orthogonal transformation too and has several advantages over other traditional VIs (Crist and Cicone 1984b; Kauth and Thomas 1976).

The TCT has revolutionized the concept of understanding the plant growth patterns in spectral space formed by different bands combination (Kauth and Thomas 1976). Later, it was employed to understand the soil moisture and other hydrological features. The propounders of TCT used MSS data to investigate the plant growth patterns in connection with 'triangular cap-shaped region with a tassel' in red–NIR space (Kauth and Thomas 1976; Ray 1994). The top of their tasselled cap with low red reflectance and higher NIR reflectance was found representative of higher vegetated areas, while the opposite to the top, the flat side of the cap (not perfectly horizontal), was found representative of the bare soil (Ray 1994). The encapsulation of physical scene characteristics in the form of tasselled space has made TCT a useful index and as an investigative tool in the field of phenology and ecology (Lobser and Cohen 2007). The evolution of TCT is indebted to the profound research work done by EP Crist using both the satellite sensors like Landsat thematic mapper (TM) and spectrometer reflectance factor data for investigating crop development (Crist and Cicone 1984a). These series of findings became very helpful in determining the crop condition and landcover classification (Oetter et al. 2001; Dymond, Mladenoff, and Radeloff 2002; Cohen and Spies 1992; Cohen, Spies, and Fiorella 1995; Skakun, Wulder, and Franklin 2003). These were performed not only by using Landsat data but also through several newly developed sensors such as MODIS, QuickBird and IKONOS (Yarbrough, Easson, and Kuszmaul 2005; Zhang et al. 2002; Horne 2003).

Both multi- and hyperspectral data have highly correlated bands. TCT not only compresses several bands into few bands but also decorrelates them by transforming them orthogonally into a new set of axes associated with physical features. Traditionally, three axes were defined: (I) Brightness, (II) Greenness and (III) Wetness. Firstly, a rotation was defined to separate the vegetation from non-vegetated features by maintaining the orthogonal property between I and II components. Then, rotating components II and III orthogonally separated the water from vegetation features. Finally, orthogonal rotation between components I and III was implemented in order to separate water from features of vegetation and non-vegetation (Zhang et al. 2002). Brightness – the first feature of TCT – is a weighted sum of all the bands and accounts for the most variability in the image. It is typically associated with bare or partially covered soil, natural and man-made features, and variations in topography. Greenness is a measure of the contrast between the NIR band and the visible bands due to the scattering of infrared radiation resulting from the cellular structure of green vegetation and the absorption of visible radiation by plant pigments. Soil reflectance curves (soil signatures) are represented with higher values in 'Brightness' while they are expressed in low 'Greenness' values. The third component is

orthogonal to the first two components and is associated with soil moisture, water and other moist features (Crist and Cicone 1984b; Crist and Kauth 1986; Zhang et al. 2002). There are three planes associated with these features: the plane of soils (Brightness/Wetness space), the transition zone (Greenness/Wetness space) and the plane of vegetation (Brightness/Greenness space). Pre-planting field having bare soil will be analysed best in the plane of soils. After planting, it would shift up through the transition zone towards the plane of vegetation as the crops matured and then would 'tassel out' with senescence. All these phases of plots would together form the shape of a 'tasselled cap' (Crist and Kauth 1986; Crist and Cicone 1984b; Kauth and Thomas 1976).

Until recently, there were no standards for deriving the orthogonal rotation coefficients due to the pluralistic interpretation of the tasselled cap features (Lobser and Cohen 2007). Any number of TCTs may be developed if the choice of aligning these three axes is left to the discretion of a researcher. Since the launch of Landsat 8 in 2013, it was being demanded by researchers working on vegetation how to use TCT for this new sensor in a same way they used it for other sensors. Addressing that dire need of researchers, this study is presenting the new TCT coefficients for operational land imager (OLI) in a form of this letter. To maintain the continuity among the sensors for the same tasselled cap idea originally propounded by Kauth and Thomas (1976) and investigated by Crist with other researchers (Crist and Kauth 1986; Crist 1985; Crist and Cicone 1984b, 1984a), this study uses the Procrustes rotation (PR) transformation for deriving the TCT coefficients for OLI of Landsat 8 (Andrade et al. 2007, 2004; Lobser and Cohen 2007).

2. Materials and methods

2.1. Data set used

In this study, we not only used the same areas that were used before by earlier researchers but also added some new areas to represent a wide variety of land cover types to make TCT suitable for all type of areas and climates (Table 1). It is important to mention here that the first comprehensive study to calculate TCT for TM data was conducted by Crist and Cicone (1984b) and they selected only three scenes to derive their famous TM TCT index (also shown in Table 1). Moreover, they mainly used North Carolina scene (24 September 1982) to derive these coefficients and described this scene as an ideal scene due to its diversity holding large fields surrounded by forest and water. Therefore, we used the same areas in this study not only to derive TCT for Landsat 8 but also to make new coefficients more representative of vegetation and other landcover types, and several other areas were also included to corroborate the analysis (Table 1).

The at-satellite reflectance-based TCT was derived by focusing especially on the methodology described by Crist and Cicone (1984b), Huang et al. (2002) and Lobser and Cohen (2007). Conversion from DN to reflectance was done according to the method mentioned on the website of USGS (http://landsat.usgs.gov/Landsat8_Using_Product.php). Sub-scenes were chosen from all scenes, and the regions of interest (ROIs) were defined by using high-resolution imagery of Google Earth. Crist and Cicone used 9000–13,000 pixel samples from their three sub-scenes. About 2000 random samples were selected from each of the 10 ETM + scenes by Huang et al. (2002). Approximately 1.2×10^6 pixels were randomly selected by Lobser and Cohen (2007) from their global sample of MODIS data. A simple random sample may be heavily biased due to the presence of clouds and snow, so samples generated in this work were only from those areas that were visibly not affected by clouds and snow (uneven sample size from

Table 1. Study areas.

Scene #	Path/Row	Location	Rationale for selection	Acquisition Date	Scene ID
1	121/40	Jiangxi, China	Poyang lake, urban and vegetation areas	14 May 2013	LC81210402013134
2	31/30	Northern Nebraska, South Dakota	Variety of crop fields, urban areas, airport and bare soil	23 May 2013	LC80310302013143
3	16/34	West Virginia	Mountainous forests, water bodies and urban features	30 May 2013	LC80160342013150
4	16/34	West Virginia	Mountainous forests, water bodies and urban features	15 June 2013	LC80160342013166
5	16/35	North Carolina	Agricultural holdings, forest and water bodies	15 June 2013	LC80160352013166
6	39/31	Idaho	Large water bodies and crop fields	16 June 2013	LC80390312013167
7	121/40	Jiangxi, China	Poyang lake, urban and vegetation areas	1 July 2013	LC81210402013182
8	39/31	Idaho	Large water bodies and crop fields	2 July 2013	LC80390312013183
9	152/41	Indus River Basin	Indus River, extensive crop fields	10 July 2013	LC81520412013191
10	152/41	Indus River Basin	Indus River, extensive crop fields	27 August 2013	LC81520412013239

different scenes). We chose a random sample comprising 0.2% (24,371 pixels) for West Virginia scene, 1% (8510 pixels) for North Carolina scene and 10% (64,000 pixels) for Idaho scene to rotate axes orthogonally by using principal component analysis (PCA). Remaining seven scenes were used for the sake of corroboration. In this way, six orthogonal axes were generated and among which first three axes were used to transform data by using PR method (Mardia, Kent, and Bibby 1979; Lobser and Cohen 2007; Andrade et al. 2007, 2004).

2.2. *Tasselled cap transformation method*

For a sensor carrying four bands, Gram–Schmidt orthogonalization is used (Huang et al. 2002; Crist and Cicone 1984b; Kauth and Thomas 1976). For higher number of bands, after applying PCA, all three axes are rotated to separate different features from each other. It has been found that there is no standard mechanism in literature currently available for this post-PCA rotation, and thus rotation is subjected to interpretation (Lobser and Cohen 2007). Lobser and Cohen (2007) attempted to standardize derivation of transformation coefficients for future sensors. By following the standard developed by them, the below-mentioned approaches were followed:

(1) Firstly, dummy target was generated by applying Landsat TM TCT coefficients on Landsat 8 data.

(2) Then, by using PR method, PCA transformed Landsat 8 data were rotated for the best alignment to the dummy target.
(3) Finally, simple multiplication was done between the transformation coefficients developed through Procrustes and PCA coefficients to get the final TCT coefficients for Landsat 8.

Although these components are ultimately rotated, the 3D structure of the data space is retained through this rotation. Thus, the final transformation is highly dependent upon the chosen starting dummy target.

2.3. *Principal component analysis*

PCA maximizes variance while minimizing correlation by means of an orthogonal transformation (Mardia, Kent, and Bibby 1979). The resulting uncorrelated PC bands are linear combinations of the original spectral bands. The first few PC bands normally represent the 90–96% variance in the data, and the remaining bands represent noise (Mardia, Kent, and Bibby 1979). In this study, PCA is applied on the random samples representing the vegetation, soil, water and other landcover features to generate the new components in orthogonal space. All of these new orthogonal components are used in PR.

2.4. *Procrustes rotation*

In multivariate statistics, PR is based on singular value decomposition (SVD) to decompose a matrix into principal components for simultaneous comparison of several data sets (Andrade et al. 2007). 'Procrustes rotation is usually performed on the principal components that describe the data instead of on the data itself' (Andrade et al. 2004). The main idea of PR is based on comparing two or more spaces where the same variables are measured. Here, PR is applied on PCA-transformed axes to transform the orthogonal space in best conformation to the dummy target space based on TM TCT space.

3. Results and discussion

By following the methodology mentioned above, TCT coefficients are derived for different landcover types in different time periods to make the derived scenes representative of all sorts of important features. A 2D scatter plot for both Red and NIR channels can be seen in Figure 1(*a*). The diagonal in this distribution is termed as a 'soil line'. This soil line in spectral space describes the variation in the spectrum of bare soil in the selected area. In any image showing the pattern like Figure 1(*a*), this line can be found by locating two or more patches of bare soil having different values of reflectance and finding the best fit line in spectral space (Ray 1994; Viña et al. 2011; Payero, Neale, and Wright 2004; Bannari et al. 1995; Gitelson et al. 2002).

Figure 1(*b*) is confirming the concept of 'triangular cap-shaped region with a tassel' in red–NIR space, which was put forward by Kauth and Thomas using MSS data. They found that the point of the cap (which lies at low red reflectance and high NIR reflectance) represented regions of high vegetation and that the flat side of the cap directly opposite the point represented bare soil (Kauth and Thomas 1976).

Table 2 shows the transformation coefficients for Landsat 8 at-satellite reflectance data. These coefficients are very close to the coefficients of the dummy target image created through TM-based TCT coefficients. From Table 2, it is evident that Brightness

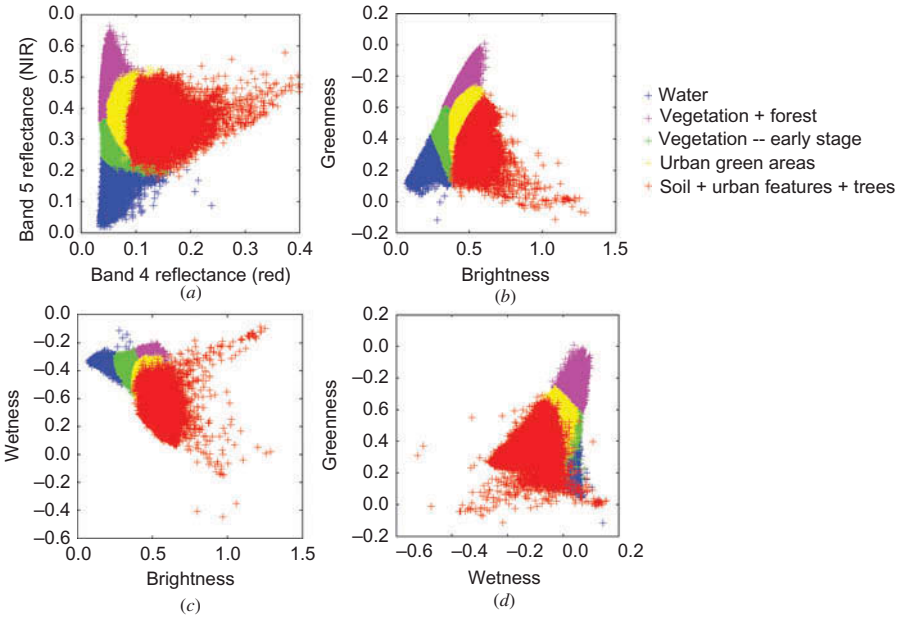

Figure 1. (*a*) Scatter plot between Red (band 4) and NIR bands (band 5) along with all five regions of interests (ROIs); (*b*) Scatter plot between Brightness and Greenness. It is also called 'plane of vegetation'; (*c*) Scatter plot between Brightness and Wetness. It is also termed as 'plane of soil'; (*d*) Scatter plot between Wetness and Greenness. It is called as 'transition zone'.

Table 2. TCT coefficients for Landsat 8 at-satellite reflectance.

Landsat 8 TCT	(Blue) Band 2	(Green) Band 3	(Red) Band 4	(NIR) Band 5	(SWIR1) Band 6	(SWIR2) Band 7
Brightness	0.3029	0.2786	0.4733	0.5599	0.508	0.1872
Greenness	−0.2941	−0.243	−0.5424	0.7276	0.0713	−0.1608
Wetness	0.1511	0.1973	0.3283	0.3407	−0.7117	−0.4559
TCT4	−0.8239	0.0849	0.4396	−0.058	0.2013	−0.2773
TCT5	−0.3294	0.0557	0.1056	0.1855	−0.4349	0.8085
TCT6	0.1079	−0.9023	0.4119	0.0575	−0.0259	0.0252

has all positive loadings. It means that all six bands contribute for its overall value with bands 4 (Red), 5 (NIR) and 6 (SWIR1) as maximum contribution. Regions of high vegetation are found at low Red and higher NIR regions and here (Table 2) both have higher values of loadings, so any increase in vegetation density will cause less substantial changes in Brightness. It indicates that this feature will be responsive to soil characteristics including its albedo instead of vegetation.

The fact that vegetation has higher values of reflectance in NIR while lower in Red regions of the (electromagnetic) spectrum is displayed by the loadings corresponding to Greenness in Table 2. Here, Greenness has high positive loadings in NIR while high negative loadings in Red spectra (Figure 1(*b*)).

When the third feature, i.e. 'Wetness' is analysed, Table 2 shows that it contrasts the sum of the visible and NIR bands with the sum of the SWIR bands. The SWIR bands are considered to be the most sensitive to both soil moisture and plant moisture, so the contrast between these two sets of bands mainly highlights moisture-related scene characteristics (Figure 1(*c*)) (Crist and Cicone 1984b).

On the basis of these characteristics of Brightness, Greenness and Wetness, Figures 1 (*b–d*) show the planes between first three transformations. The plane between Brightness and Greenness is considered as a plane of vegetation, while the plane between Brightness and Wetness is considered as a plane of soils (Crist and Cicone 1984b).

These three planes (Figures 1 (*b–d*)) are in accordance with those three planes constructed for Landsat TM TCT space by Crist and Cicone (Crist and Kauth 1986; Crist and Cicone 1984b). Thus, using the standard approach to derive the coefficients for a new sensor gives the same TCT space developed by TCT pioneers and thus provides the data continuity for studying the phenology and analysing the temporal series for vegetation change or biomass variation.

4. Conclusions

TCT compresses and decorrelates the data into few bands associated with physical scene characteristics of the land surface. Brightness, Greenness and Wetness are those few important components mostly discussed in literature. Brightness is related to the soil and albedo, Greenness is associated with vegetation and Wetness is mostly connected with water contents. As transformation solely depends upon the interpretation of the data, standardization was necessary to develop uniformity in the TCT based on Landsat MSS, TM and ETM + sensors as well as those based on the new sensors. This study investigated the method using TM-based TCT coefficients to simulate OLI image to be used as a dummy target in PR method for transforming OLI orthogonal space. The resulted transformation coefficients successfully differentiated soil from vegetation, vegetation from water and bare soil features from water features. The standardized approach used in this study has a great potential for deriving coefficients for future sensors such as Sentinel-2, etc. Validation of coefficients will be done in a form of a comparison with ETM + in a detailed next paper.

Acknowledgements

We would like to thank Prof. Bruce Wylie from USGS and Prof. W.B. Cohen from Oregon State University for their useful feedback during this research process. We are indebted to Dr. Mohtashim H. Shamsi from the University of Toronto, Mr. Qin Bangyong and Mr. Jiang Gaozhen for their valuable contribution. Last but not least, we owe debt of gratitude to the Editor, two unknown reviewers and the administrative assistant of RSL for giving us very important feedback to improve the quality of this letter.

Funding

This work was funded by the National Natural Science Foundation of China [grant numbers 41371362, 41371359 and 41201348].

References

Andrade, J. M., M. Kubista, A. Carlosena, and D. Prada. 2007. "3-Way Characterization of Soils by Procrustes Rotation, Matrix-Augmented Principal Components Analysis and Parallel Factor Analysis." *Analytica Chimica Acta* 603 (1): 20–29. doi:10.1016/j.aca.2007.09.043.

Andrade, J. M., M. P. Gómez-Carracedo, W. Krzanowski, and M. Kubista. 2004. "Procrustes Rotation in Analytical Chemistry, a Tutorial." *Chemometrics and Intelligent Laboratory Systems* 72 (2): 123–132. doi:10.1016/j.chemolab.2004.01.007.

Bannari, A., D. Morin, F. Bonn, and A. R. Huete. 1995. "A Review of Vegetation Indices." *Remote Sensing Reviews* 13 (1–2): 95–120. doi:10.1080/02757259509532298.

Clevers, J. G. P. W. 1988. "The Derivation of a Simplified Reflectance Model for the Estimation of Leaf Area Index." *Remote Sensing of Environment* 25 (1): 53–69. doi:10.1016/0034-4257(88)90041-7.

Cohen, W. B., and T. A. Spies. 1992. "Estimating Structural Attributes of Douglas-Fir/Western Hemlock Forest Stands from Landsat and SPOT Imagery." *Remote Sensing of Environment* 41 (1): 1–17. doi:10.1016/0034-4257(92)90056-P.

Cohen, W. B., T. A. Spies, and M. Fiorella. 1995. "Estimating the Age and Structure of Forests in A Multi-Ownership Landscape of Western Oregon, USA." *International Journal of Remote Sensing* 16 (4): 721–746. doi:10.1080/01431169508954436.

Crist, E. P. 1985. "A TM Tasseled Cap Equivalent Transformation for Reflectance Factor Data." *Remote Sensing of Environment* 17 (3): 301–306. doi:10.1016/0034-4257(85)90102-6.

Crist, E. P., and R. C. Cicone. 1984a. "Comparisons of the Dimensionality and Features of Simulated Landsat-4 MSS and TM Data." *Remote Sensing of Environment* 14 (1–3): 235–246. doi:10.1016/0034-4257(84)90018-X.

Crist, E. P., and R. C. Cicone. 1984b. "A Physically-Based Transformation of Thematic Mapper Data-the TM Tasseled Cap." *IEEE Transactions on Geoscience and Remote Sensing*, GE–22 (3): 256–263. doi:10.1109/Tgrs.1984.350619.

Crist, E. P., and R. J. Kauth. 1986. "The Tasseled Cap De-Mystified." *Photogrammetric Engineering and Remote Sensing* 52 (1): 81–86.

Dymond, C. C., D. J. Mladenoff, and V. C. Radeloff. 2002. "Phenological Differences in Tasseled Cap Indices Improve Deciduous Forest Classification." *Remote Sensing of Environment* 80 (3): 460–472. doi:10.1016/S0034-4257(01)00324-8.

Gitelson, A. A., R. Stark, U. Grits, D. Rundquist, Y. Kaufman, and D. Derry. 2002. "Vegetation and Soil Lines in Visible Spectral Space: A Concept and Technique for Remote Estimation of Vegetation Fraction." *International Journal of Remote Sensing* 23 (13): 2537–2562. doi:10.1080/01431160110107806.

Horne, J. H. 2003. "A Tasseled Cap Transformation for IKONOS Images." In *ASPRS 2003 Annual Conference Proceedings*, Anchorage, AK, May 3–9, 1–7. Bethesda, MD: American Society of Photogrammetry and Remote Sensing.

Huang, C., B. Wylie, L. Yang, C. Homer, and G. Zylstra. 2002. "Derivation of a Tasselled Cap Transformation Based on Landsat 7 At-Satellite Reflectance." *International Journal of Remote Sensing* 23 (8): 1741–1748. doi:10.1080/01431160110106113.

Huete, A. R. 1988. "A Soil-Adjusted Vegetation Index (Savi)." *Remote Sensing of Environment* 25 (3): 295–309. doi:10.1016/0034-4257(88)90106-X.

Huete, A. R., R. D. Jackson, and D. F. Post. 1985. "Spectral Response of a Plant Canopy with Different Soil Backgrounds." *Remote Sensing of Environment* 17 (1): 37–53. doi:10.1016/0034-4257(85)90111-7.

Jackson, R. D., and A. R. Huete. 1991. "Interpreting Vegetation Indices." *Preventive Veterinary Medicine* 11 (3–4): 185–200. doi:10.1016/S0167-5877(05)80004-2.

Jordan, C. F. 1969. "Derivation of Leaf Area Index from Quality of Light on the Forest Floor." *Ecology* 50: 663–666. doi:10.2307/1936256.

Kauth, R. J., and G. S. Thomas. 1976. "The Tasselled Cap—A Graphic Description of the Spectral-Temporal Development of Agricultural Crops as Seen by Landsat." Paper presented at the LARS Symposia, Proceedings of the Symposium on Machine Processing of Remotely Sensed Data, Purdue University, West Lafayette, IN, June 29–July 1, 4B41–4B51.

Lobser, S. E., and W. B. Cohen. 2007. "MODIS Tasselled Cap: Land Cover Characteristics Expressed through Transformed MODIS Data." *International Journal of Remote Sensing* 28 (22): 5079–5101. doi:10.1080/01431160701253303.

Mardia, K. V., J. T. Kent, and J. M. Bibby. 1979. *Multivariate Analysis*. London: Academic Press.

Oetter, D. R., W. B. Cohen, M. Berterretche, T. K. Maiersperger, and R. E. Kennedy. 2001. "Land Cover Mapping in an Agricultural Setting Using Multiseasonal Thematic Mapper Data." *Remote Sensing of Environment* 76 (2): 139–155. doi:10.1016/S0034-4257(00)00202-9.

Payero, J. O., C. M. U. Neale, and J. L. Wright. 2004. "Comparison of Eleven Vegetation Indices for Estimating Plant Height of Alfalfa and Grass." *Applied Engineering in Agriculture* 20 (3): 385–393. doi:10.13031/2013.16057.

Ray, T. W. 1994. "A FAQ on Vegetation in Remote Sensing." Accessed March 23, 2014. http://www.yale.edu/ceo/Documentation/rsvegfaq.html.

Richardson, A. J., and J. H. Everitt. 1992. "Using Spectral Vegetation Indices to Estimate Rangeland Productivity." *Geocarto International* 7: 63–69. doi:10.1080/10106049209354353.

Richardson, A. J., and C. L. Wiegand. 1977. "Distinguishing Vegetation from Soil Background Information." *Photogrammetric Engineering and Remote Sensing* 43 (12): 1541–1552.

Rouse, J. W., R. H. Haas, J. A. Schell, and D. W. Deering. 1973. "Monitoring Vegetation Systems in the Great Plains with ERTS." In *Paper presented at the Third ERTS Symposium, NASA SP-351*, Vol. I, December 10–14, 309–317. Washington, DC: NASA.

Skakun, R. S., M. A. Wulder, and S. E. Franklin. 2003. "Sensitivity of the Thematic Mapper Enhanced Wetness Difference Index to Detect Mountain Pine Beetle Red-Attack Damage." *Remote Sensing of Environment* 86 (4): 433–443. doi:10.1016/S0034-4257(03)00112-3.

Viña, A., A. A. Gitelson, A. L. Nguy-Robertson, and Y. Peng. 2011. "Comparison of Different Vegetation Indices for the Remote Assessment of Green Leaf Area Index of Crops." *Remote Sensing of Environment* 115 (12): 3468–3478. doi:10.1016/j.rse.2011.08.010.

Yarbrough, L. D., G. Easson, and J. S. Kuszmaul. 2005. "QuickBird 2 Tasseled Cap Transform Coefficients: A Comparison of Derivation Methods." In *Paper presented at Pecora 16 "Global Priorities in Land Remote Sensing",* Sioux Falls, October 23–27. http://www.asprs.org/a/conference-archive/pecora16/.

Zhang, L. S., S. Furumi, K. Muramatsu, N. Fujiwara, M. Daigo, and L. Zhang. 2007. "A New Vegetation Index Based on the Universal Pattern Decomposition Method." *International Journal of Remote Sensing* 28 (1): 107–124. doi:10.1080/01431160600857402.

Zhang, X. Y., C. B. Schaaf, M. A. Friedl, A. H. Strahler, F. Gao, and J. C. F. Hodges. 2002. "MODIS Tasseled Cap Transformation and its Utility." In *Proceedings of IEEE International Geoscience and Remote Sensing Symposium (IGARSS'02)*, Vol. 2, Toronto, ON, June 24–28, 1063–1065. Piscataway, NJ: IEEE. doi: 10.1109/IGARSS.2002.1025776.